Q. J. R. Meteorol. Soc. (2000), **126**, pp. 899–924

Atmospheric and surface variations during westerly wind bursts in the tropical western Pacific

By JOHN FASULLO* and PETER J. WEBSTER
University of Colorado at Boulder, USA

(Received 30 October 1997; revised 6 April 1999)

SUMMARY

An analysis is made of variations in both the surface energy balance and the regional atmospheric dynamic and thermal structure during 44 westerly wind bursts (WWBs) in the western equatorial Pacific Ocean from 1979 to 1995. The study assesses winds, convective available potential energy, cloud properties, precipitation, surface temperature, and surface heat flux while distinguishing between brief (5–25 day periodicity) and sustained (30–90 day) WWBs. Datasets used in the study include fields from the NCEP/NCAR and ECMWF re-analyses, and satellite retrievals of clouds (ISCPP), precipitation (MSU), moisture (TOVS), and surface solar flux.

Both brief and sustained WWBs, by definition, experience strong low-level westerly winds that typically induce an increased surface latent-heat flux of approximately 30 W m^{-2}. Enhanced cloud thickness, precipitation, and upper tropospheric easterly wind anomalies accompany surface westerly winds, though maxima in winds lag those in clouds and precipitation by about one day for brief WWBs and four days for sustained events. WWBs of both types experience strong seasonality, occurring frequently in all seasons except boreal summer.

Important distinctions between brief and sustained WWBs can also be made. Westerly anomalies typically extend above 200 hPa during brief WWBs but are generally confined to the lower troposphere (below 400 hPa) for sustained events. Sustained WWBs are also preceded by a quiescent period of reduced cloud thickness and surface winds that is accompanied by strong incident solar flux. Convective instability, as judged by a variety of techniques, increases by approximately 30% during this quiescent period. Brief WWBs do not include the precursory surface warming or convective destabilization of sustained WWBs. Notwithstanding the warming episodes before the events, sustained WWBs are associated with a net surface cooling approximately 40% larger than brief WWBs.

The relationship between brief and sustained WWBs and the phase of the Madden–Julian Oscillation (MJO) (as judged from outgoing long-wave radiation) is also examined. Results support the classification of events as 'brief' and 'sustained' as used in this study, with brief WWBs occurring frequently during both wet and dry phases of the MJO, while sustained WWBs occur uniquely during the MJO wet phase. The association of brief and sustained WWBs with the MJO is shown to be independent of the El Niño Southern Oscillation phase. It is therefore proposed that some, but not all, WWBs may be viewed as the surface signature of the MJO and that the mechanisms responsible for the MJO play an integral role in the formation and sustenance of sustained WWBs.

KEYWORDS: Convection Madden–Julian Oscillation Tropical dynamics

1. INTRODUCTION

Westerly wind bursts (WWBs) are unique features of the tropical western Pacific Ocean and play a critical role in the maintenance of the warm pool and creation of equatorial waves and currents (e.g. Knox and Halpern 1982; McPhaden *et al.* 1988). Over the warm pool, WWBs modify strongly air–sea fluxes of heat and momentum (e.g. McPhaden *et al.* 1988; Young *et al.* 1992) and are associated with deep convection and periods of intense rainfall and ocean mixing. The events thus have a strong impact on atmospheric heating, surface fresh water flux, and upper-ocean stability. Moreover, the increased surface stress during WWBs induces deflections in the oceanic thermocline that propagate eastwards into the central Pacific (e.g. Wyrtki 1975) and influence remotely the sea surface temperature (SST) field. WWBs are therefore an important element of the El Niño Southern Oscillation (ENSO). The diversity of roles for WWBs, in both a local and a large-scale context, highlights the need for a comprehensive understanding of the events.

Detailed studies of WWBs have been hindered by a lack of high-quality data and a limited number of observations. Most analyses have focussed on case-studies of individual WWBs such as those during the Winter Monsoon Experiment (Williams

* Corresponding author: PAOS, CB 311, University of Colorado, Boulder, CO 80309, USA.

1981), at the onset of the 1982–83 El Niño (Chu and Frederick 1990), and accompanying twin cyclone pairs (Lander and Morrissey 1988). These studies reveal the highly variable nature of WWBs. For example, Hartten (1996) concludes that WWBs are rarely associated with twin cyclone pairs and identifies a variety of synoptic settings in which WWBs are observed to occur. Similarly, Harrison and Vecchi (1997) identify eight different types of WWBs as a function of location within the tropical Pacific. Also, an extended climatology of WWBs was examined by Harrison and Giese (1991) using island surface wind observations over a broad latitudinal and longitudinal domain from 1950 to 1980. Their results show WWBs to be highly variable on seasonal and interannual time-scales, occurring most often in boreal winter and spring, and displaced eastwards during warm ENSO conditions.

Despite the wide variety of synoptic settings and geographical locations for WWBs, attempts to explain the existence of WWBs have typically examined a single set of processes. For example, the root cause of WWBs was initially attributed to propagation of cold surges from higher latitudes into the tropics (e.g. Chang and Lau 1982; Arkin and Webster 1985). Modelling and diagnostic studies of extratropical–tropical interactions suggest that such interactions do exist and that this interaction may be an important root cause of some bursts (e.g. Williams 1981; Lim and Chang 1981; Arkin and Webster 1985; Kiladis *et al.* 1994). However, other bursts appear to be independent of the higher-latitude forcing (Compo *et al.* 1999). Additionally, the vertical structure of WWBs has been observed to vary significantly (Gutzler *et al.* 1994) and their coincidence with enhanced clouds and precipitation, while evident and well documented, can vary in phase, magnitude, and duration (Gutzler *et al.* 1994). It is also known that WWBs occur more frequently in the convective phase of the Madden–Julian Oscillation (MJO, Madden and Julian 1972, 1994; Nitta and Motoke 1987; Lander and Morrissey 1988; Murakami and Sumathipala 1989). The precise relationship between WWBs and the MJO has not been well characterized, however, and despite the above mentioned efforts a generalized framework that classifies WWBs, while allowing for their large observed variability, has yet to be established.

In the context of ocean–atmosphere interactions within the warm pool, WWBs are significant because they alter surface heat and momentum fluxes (McPhaden *et al.* 1988, 1992; Lukas and Lindstrom 1991) and induce a significant degree of oceanic fresh-water mixing following sustained precipitation events. Both local (Luther *et al.* 1983; Lukas *et al.* 1984; Eriksen 1993) and remote (Knox and Halpern 1982; Hendon *et al.* 1998) oceanic responses have been documented following impulsive forcing by WWBs. In analysis of the surface energy balance, it has been generally assumed that evaporative effects dominate variations in other heat-flux terms (e.g. McPhaden *et al.* 1988, 1992); however, comprehensive studies of the surface energy balance during WWBs are rare. Sub-surface temperature changes in the ocean are known to be the result of dynamic influences. McPhaden *et al.* (1992) demonstrate the warming influence of WWBs on deeper levels of the upper ocean (150 m) by changes in the meridional Ekman convergence and zonal convergence. Deep turbulent mixing has also been shown to be responsible for subsurface warming (Lukas and Lindstrom 1991). Enhanced surface momentum fluxes modulate currents, causing eastward acceleration of over 1 m s^{-1} at the surface and westward acceleration at 150 m of about 40 cm s^{-1}. Opposing the processes that mix the upper ocean, strong precipitation in the early stages of WWBs can enhance oceanic stability (Webster and Lukas 1992).

Several studies have suggested an important role for WWBs in modifying eastern Pacific SST through Kelvin waves (Wyrtki 1975; Harrison and Schopf 1984; Lukas

et al. 1984). These eastwardly propagating waves deepen the mixed layer, reduce entrainment with the deep ocean, and generally extend the warm pool eastwards. Knox and Halpern (1982) provide direct evidence for the 2–3 month propagation period of Kelvin waves across the Pacific basin following excitation by westerly bursts. These findings are substantiated by results from the TOGA-COARE* (Godfrey *et al.* 1995). Also, Hendon *et al.* (1998) demonstrate that surface westerly winds associated with the lower-frequency components of the MJO and the gravest baroclinic oceanic Kelvin wave comprise a near resonant forcing in the warm-pool regions, and can play an important role in modifying equatorial Pacific SST. Hendon *et al.* (1998) also demonstrate that the oceanic response depends strongly on the spatial extent, latitudinal displacement, and propagation speed of the anomalies. Thus, an important question exists regarding whether the processes that determine the nature of surface wind anomalies during some events (e.g. MJO) are characteristic of WWBs as a group.

The principal aim of the current study is to develop a framework for the understanding of WWBs that addresses their dynamic and thermal structure, and their associations with clouds, precipitation, and convective instability, while considering the apparently high degree of variability among WWBs. The study covers a 17-year period of data recently provided by the National Centers for Environmental Prediction/National Center for Atmospheric Research (NCEP/NCAR) in conjunction with more brief datasets from the European Centre for Medium-Range Weather Forecasts (ECMWF) 15-year re-analysis project and several satellite projects. The large number of events sampled by the data allows distinctions between events to be made based on their spatial and temporal scales, and it will be shown that the scales identified comprise an important basis for distinguishing among WWBs. A comprehensive assessment of surface latent, sensible, and radiative heat-flux anomalies during each type of WWB will also be made.

2. Data, WWB identification, and derived fields

During the TOGA decade (1985–94), extensive monitoring of the coupled ocean–atmosphere system began with the establishment of the Tropical Ocean Atmosphere buoy array in the tropical Pacific Ocean and an enhancement of surface and upper-atmosphere observations extended around the tropical oceans (World Meteorological Organization 1985; World Climate Research Programme 1990). Datasets from the NCEP/NCAR (Kalnay *et al.* 1995) and ECMWF (Gibson *et al.* 1997) re-analysis projects incorporate much of these monitored data in their assimilation. Those fields most strongly influenced by observations during the assimilation process, such as winds, temperature, and humidity, will be examined in this analysis. As surface turbulent fluxes depend heavily on wind speed, flux estimates from the re-analysis also compare favourably with *in-situ* observations, and their appropriateness for the current analysis will be discussed further in section 2(a). However, as observations of clouds and precipitation are not included in the model assimilation (Kalnay *et al.* 1995), alternative data sources will also be considered. Cloud characteristics from the International Satellite Cloud Climatology Project (ISCCP) C1 dataset (Rossow and Schiffer 1991) and precipitation estimates based on Microwave Sounder Unit (MSU) satellite retrievals (Spencer 1993) blended with surface gauge measurements (Magana *et al.* 1998) are assessed. Temperature and precipitable water estimates are taken from the TIROS† Operational Vertical Sounder (TOVS, Smith *et al.* 1979) analysis product produced by the National

* The Coupled Ocean–Atmosphere Response Experiment of the Tropical Ocean and Global Atmosphere programme (World Climate Research Programme).

† Television Infra-Red Observation Satellite.

TABLE 1. THE TEMPORAL EXTENT AND SAMPLING CHARACTERISTICS OF THE DATASETS USED

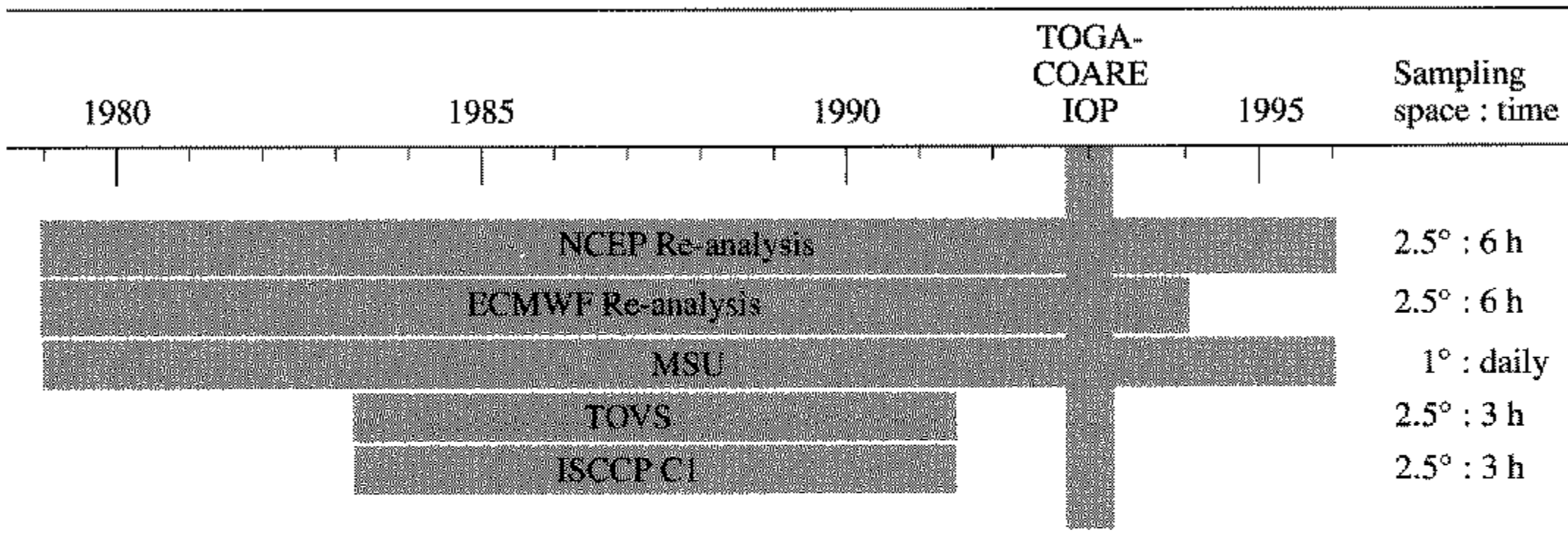

See text for explanation of the acronyms.

Oceanic and Atmospheric Administration (NOAA) to cross-check re-analysis moisture fields. The TOVS product allows an estimation of variability of temperature and moisture independent of the re-analysis models' physics but is limited by its temporal sampling rate and its coarse vertical resolution.

(*a*) *Data product evaluation*

The characteristics of the datasets used in the current study are summarized in Table 1. The Table shows the temporal extent of each dataset and the spatial and temporal resolution of its reported fields. In these compiled datasets, however, raw observations are typically made over finer spatial and temporal scales than the reported fields. For example, radiances from the MSU over the tropics are made twice per day (0600 and 1800 GMT) but are reported daily. Moreover, datasets derived from multiple fields, such as the re-analyses and ISCCP cloud properties, result from a blend of observations with distinct sampling times and spatial scales. The number and type of raw observations included in fields such as the re-analysis and precipitation estimates can be a strong function of location and time. Moreover, some fields are derived solely from model parametrizations (e.g. surface heat fluxes) and observations of those fields are not included in the model assimilation. Thus, even though the datasets appear to be individually homogeneous, there are questions of consistency that must be addressed about their use in tandem and about their representativeness of nature, in general. To help verify the accuracy of the datasets used, therefore, comparisons will be made with observations during the TOGA-COARE Intensive Observing Period (IOP) which extended from 1 November 1992 to 28 February 1993.

Figure 1 shows a comparison between datasets used in the current analysis and measurements from the Woods Hole Improved Meteorology (IMET) buoy at 156°E, 1.45°S and the R/V *Moana Wave*, which together surveyed meteorological conditions during the TOGA-COARE IOP. Re-analysis zonal wind estimates (Fig. 1(a)) correlate strongly with observations at 0.90 and 0.88 for the ECMWF and NCEP/NCAR re-analysis, respectively, and bias among the estimates is approximately 0.1 m s^{-1}. The close agreement in wind fields is consistent with the strong influence of assimilated wind data on the re-analysis fields as noted by Kalnay *et al.* (1995). Surface turbulent fluxes, however, are derived solely from model parametrizations. Figure 1(b) shows the correlation between surface latent flux as calculated by Fairall *et al.* (1996) from bulk formulations for three cruises of the R/V *Moana Wave* and fields from the ECMWF and NCEP/NCAR re-analysis. Latent-flux observations and re-analysis fields correlate

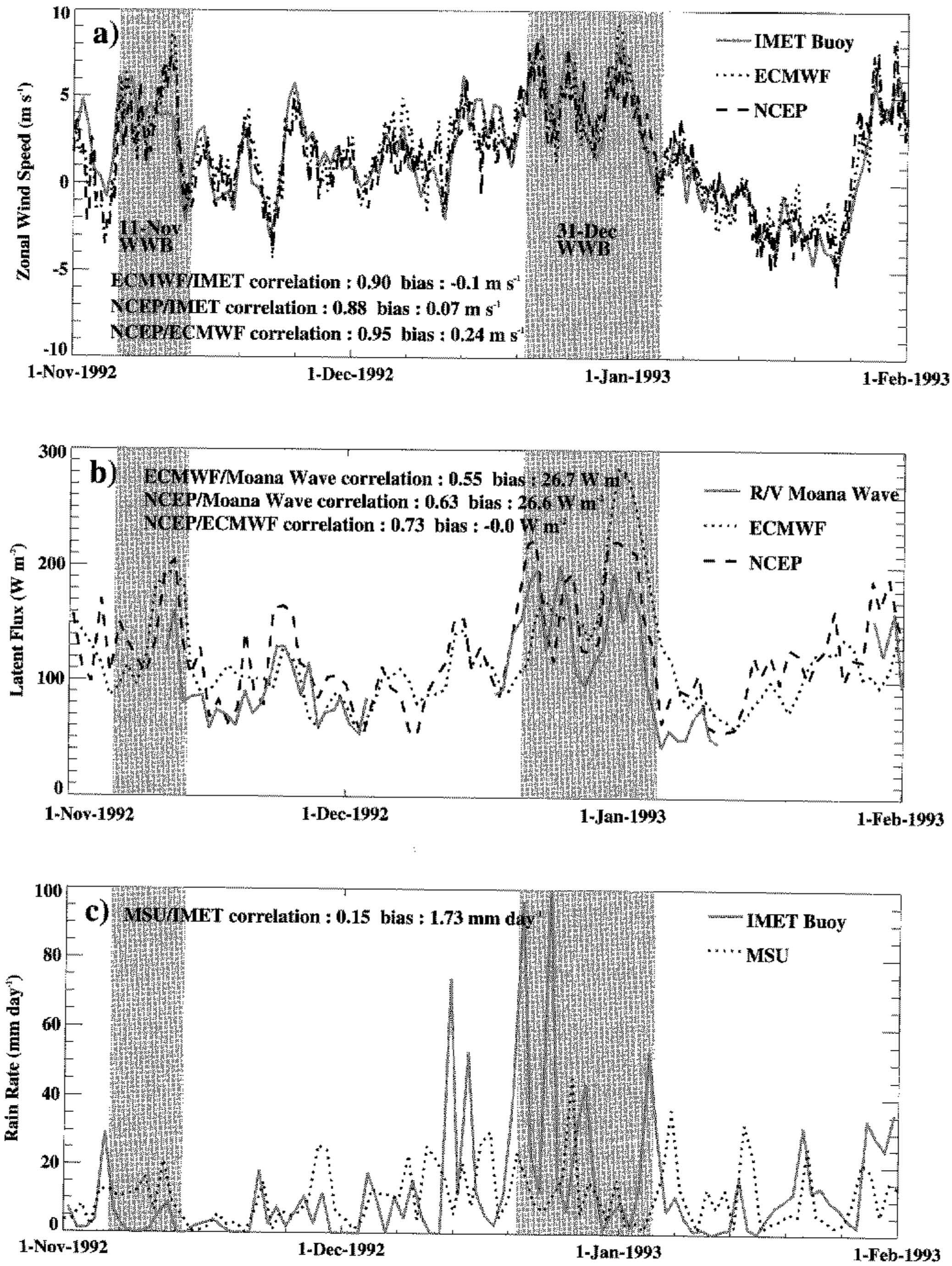

Figure 1. Comparison of estimates of meteorological surface variables from ECMWF and NCEP/NCAR re-analysis estimates and satellite Microwave Sounder Unit (MSU) retrievals with observations from the IMET buoy and the R/V *Moana Wave* during the TOGA-COARE intensive observating period. (a) surface (3 m buoy, 1000 mb re-analyses) zonal wind, (b) surface latent flux, and (c) precipitation. Shaded areas show the periods of the two westerly wind bursts (WWB).

well, though disagreement between the fields is somewhat greater than for winds. Some disagreement may result from the disparity of analysis scales. Nonetheless, the re-analysis latent-flux estimates are sufficient to quantify the strong increase in evaporation associated with WWBs, such as the elevated fluxes in late December 1992. A larger discrepancy between observations and the data record is evident in comparison of MSU derived precipitation and the IMET buoy record in Fig. 1(c), however. The data do not compare well on a daily basis but transitions from dry to rainy episodes on weekly time-scales, such as the extended dry period in November and the increase in precipitation during December, appear to be represented by both. Again, some disagreement between the estimates may result from a mismatch of spatial scales, and absolute error in the MSU estimates is therefore difficult to quantify. MSU rainfall estimates will therefore only be used in this analysis to distinguish qualitatively between suppressed and enhanced rainfall transitions on weekly time-scales.

(*b*) *WWB identification*

A principal objective of the present analysis is to develop a framework around which the WWBs from the data record in Fig. 1(a) can be interpreted. Studies of WWBs have commonly defined events as large-scale occurrences of strong low-level westerly winds in excess of 5 m s^{-1}; both WWBs in Fig. 1 meet this criterion. However, it has also been recognized that a single classification of WWBs may not be appropriate due to differences in the large-scale circulation with which the events are associated (e.g. Kiladis *et al.* 1994). Moreover, the data record from the TOGA-COARE (Fig. 1) suggests different phase relationships between winds, precipitation, and surface fluxes for the brief WWB at 11 November 1992, and the sustained event which peaks on 31 December 1993. Though both WWBs are associated with enhanced fluxes and rainfall, the early (11 November) WWB occurs simultaneously with enhanced precipitation while the later event (31 December) is preceded by precipitation anomalies by approximately a week. Also, Gutzler *et al.* (1994) show contrasting vertical structure for the two events as westerlies during the early event extend deep into the troposphere while the later event is accompanied by shallow westerlies and strong easterlies aloft. Thus it appears that the sustained 31 December WWB is characterized by a strongly baroclinic structure while the 11 November WWB is nearly barotropic. Attempts to distinguish among WWBs based on a limited data record such as in Fig. 1 are not, however, definitive.

An attempt will therefore be made to assess differences between brief (5 to 25 day) and sustained (30 to 90 day) WWBs using the mean 850 hPa zonal wind in the TOGA-COARE Intensive Flux Array (IFA, Webster and Lukas 1992) which is located in the centre of the western Pacific warm pool (151°E–158°E, 5°S–2°N) as represented in the re-analysis products. The selection of distinct time bands is supported by Kiladis *et al.* (1994) who demonstrate uniqueness in the large-scale behaviour of dynamics and outgoing long-wave radiation (OLR) for WWBs delineated by these bands. It will be shown that the classification is also relevant to the variability of clouds, convective available potential energy (CAPE), temperature, and upper-ocean heat content during WWBs.

In the current analysis, WWBs are defined as events during which both the time-filtered and unfiltered mean zonal winds over the IFA exceed 3 m s^{-1}. The time filter used in the analysis is based on the Lanczos technique described by Duchon (1979) using 5479 points across the specified spectral intervals. Events meeting this criterion for any length of time are considered to be WWBs, and a temporal origin, Day 0, is

TABLE 2. TOTAL OCCURRENCE OF WESTERLY WIND BURSTS (WWBS) WITH (A) SEASON AND (B) THE PHASE OF THE MADDEN–JULIAN OSCILLATION (MJO), BASED ON THE TIME-SCALE OF FILTERED WINDS. THE MJO PHASE IS BASED ON VARIATIONS IN 30–90 DAY FILTERED OUTGOING LONG-WAVE RADIATION. (C) FREQUENCY OF EVENTS (EVENTS DAY^{-1}) DURING THE NORMAL, WARM, AND COLD PHASES OF THE NIÑO 3 REGION SEA SURFACE TEMPERATURE (SST) (5°S TO 5°N, 210°E TO 270°E) FROM 1982 TO 1995.

(a) Seasonality	December to February	March to May	June to August	September to November
Unfiltered	**35%**	26%	**7%**	32%
5–25 day	36%	24%	**8%**	32%
30–90 day	42%	**47%**	**0%**	**11%**

(b) MJO	MJO active phase	MJO inactive phase	% Events (active)
Unfiltered	42	18	**70%**
5–25 day	13	12	52%
30–90 day	18	1	**95%**

(c) Frequency vs. Niño 3 SST (WWBs week^{-1}) (% during active MJO)	Normal (272 weeks)	Warm (>0.5 degC) (213 weeks)	Cold (<−0.5 degC) (245 weeks)
Unfiltered	0.070 (**73%**)	0.085 (66%)	**0.045** (63%)
5–25 day	**0.066** (50%)	0.023 (40%)	0.033 (50%)
30–90 day	0.018 (**100%**)	0.023 (**100%**)	0.024 (**100%**)

Values with statistical significance exceeding 90% as judged by a Monte Carlo simulation are in bold. (Based on NCEP/NCAR re-analysis wind fields.)

identified for each event as the time of peak unfiltered westerly winds. Used over a fixed geographical domain, the compositing procedure has been shown to be well suited in providing a representative portrayal of WWBs (Harrison and Vecchi 1997). The focus given to events within the IFA may preclude identification of off-equatorial WWBs; however, in doing so, an emphasis is given to the WWBs most relevant to equatorial wave dynamics (e.g. Hendon *et al.* 1998).

Seasonality of WWBs and their relationship to the MJO and ENSO is summarized in Table 2(a). Both brief and sustained WWBs show strong seasonality and occur most often during boreal fall, winter, and spring, coinciding with the wet season of the Australian monsoon (January to March) and the peak in the convective signal of the MJO (Salby and Hendon 1994). However, as Table 2(b) shows, the relationship of WWBs to the MJO is a strong function of time-scale, and sustained WWBs coincide with the wet phase of the MJO (as judged from negative values of 30–90 day filtered OLR). Brief WWBs show little relationship to MJO phase, however, and occur frequently during both its wet and dry phase. The relationship between ENSO and WWBs is summarized in Table 2(c) where both the frequency of WWBs and their association with the active phase of the MJO from 1982 to 1995 are shown. WWBs identified in unfiltered data occur less often during cold ENSO conditions while brief WWBs occur more frequently during neutral ENSO conditions. The association between the frequency of sustained WWBs and the ENSO phase is not statistically distinguishable from chance based on the NCEP/NCAR data record. However, the strong association between sustained WWBs with, and the independence of, brief WWBs from the MJO is robust during all ENSO phases. It is therefore reasonable to view sustained WWBs as the surface signature of the MJO while recognizing the existence of shorter-duration events that occur independent

of the MJO phase; studies that do not distinguish between the time-scales of WWBs are likely to include a mix of these distinct phenomena.

(c) *Derived fields*

Because the lapse rate of the tropical atmosphere often approximates that of a saturated moist adiabat, a highly nonlinear relationship exists between low-level moist static energy and the energy released by convecting elements. Moist enthalpy of the lower atmosphere is therefore a poor diagnostic with which to judge the energy available for convection. Instead, CAPE is calculated to assess the role of fluctuations in low-level temperature and moisture during WWBs on clouds and stability. Calculation of CAPE assumes convective motions that originate at 1000 hPa, achieve buoyancy at the level of free convection, and convect to the altitude at which they are neutrally buoyant. Because the motions assumed by CAPE are simplistic, a generalized form of CAPE (GCAPE) is also calculated (Randall and Wang 1992). GCAPE allows convective parcels to originate at multiple levels and accounts for compensating motions in the environment. The net affect of convective motions assumed by GCAPE is to minimize the resultant enthalpy of the atmosphere. Results from CAPE and GCAPE methods are considered in tandem to judge variations in atmospheric stability during WWBs under both assumptions. It will also be shown that variability in CAPE and GCAPE estimates tend to be mutually consistent, as in the moist tropics the enthalpy of the atmosphere is often minimized by a complete condensation of moisture from the lower atmosphere such as assumed by the CAPE methodology.

3. Composite anomalies in the TOGA-COARE Intensive Flux Array

Anomalies in the above described fields are composited linearly based on the 25 brief and 19 sustained WWBs identified in winds of the NCEP/NCAR re-analysis averaged over the IFA of TOGA-COARE. Fewer events are included in the ISCCP and TOVS composites, totalling 12 and 5 for brief and sustained bursts, respectively. The temporal variability during WWBs in the depictions of the re-analysis and satellite datasets will now be presented and discussed.

(a) *Dynamic structure*

Composite raw wind anomalies in the IFA are shown in Fig. 2(a) and Fig. 2(b) for both brief and sustained WWBs with composite time-filtered data shown by Fig. 2(c) and 2(d). The climatological mean wind has been removed from the filtered time series. Brief events are characterized by westerly wind anomalies at Day 0 that extend to just over 200 hPa and cause a weakening of the mid-tropospheric easterly flow. Easterly anomalies are apparent above 200 hPa near Day 0 with the strongest anomalies occurring a day after peak surface westerly winds. The depth of westerly anomalies during brief events portrayed in the composite of re-analysis winds extends above 200 hPa which is less than during the 11 November 1992 WWB (Gutzler *et al.* 1994). In general, substantial anomalies (>1 m s^{-1}) are absent more than 15 days from Day 0 of brief WWBs.

Sustained WWBs, however, are associated with low-level westerly anomalies that extend more than 10 days from Day 0 (Fig. 2(d)). The vertical structure of dynamic anomalies is baroclinic and is consistent with observations of the sustained WWB during the TOGA-COARE (Gutzler *et al.* 1994) as strong easterly anomalies exist in the upper troposphere and westerly anomalies extend from the surface to about 350 hPa.

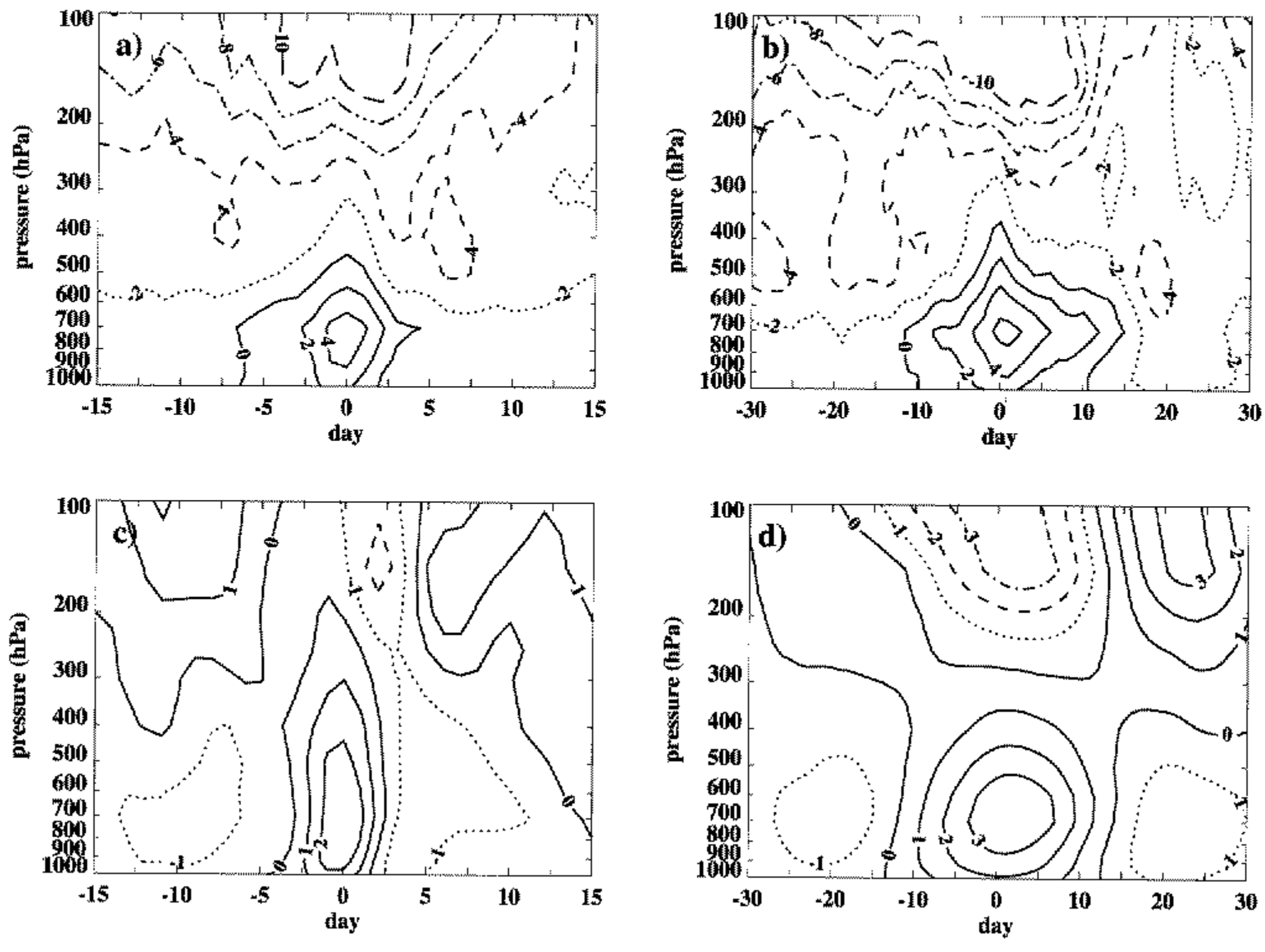

Figure 2. Cross-sections of composite zonal winds from in the intensive flux array for (a) brief and (b) sustained westerly wind bursts (WWBs) based on winds from the ECMWF re-analysis. Composites of time-filtered winds for (c) brief and (d) sustained WWBs are also shown. Dotted and dashed lines represent easterly winds.

Dynamic anomalies during sustained WWBs also include the presence of coherent low-level easterly and upper-level westerly anomalies 20 days before and following Day 0, and are consistent with classical depictions of the MJO's dynamics (e.g. Madden and Julian 1972). Low-level easterly anomalies are evident between 15 and 30 days from Day 0. It will be shown in section 3(b) that during the initial episode of anomalous low-level easterlies, an environment favourable for sustained deep convection is established, in part because of weak surface winds but also because of reduced cloudiness and high solar insolation. It will also be shown that large-scale spatial structure consistent with that of the MJO is associated with sustained WWBs (section 4). It has been shown that the spatial character of winds during WWBs is an important consideration in assessing their impact on internal oceanic waves (Hendon *et al.* 1998). At their peak, winds from the NCEP re-analysis during sustained WWBs cover an area of the western equatorial Pacific that is approximately 50% greater than at the peak of brief WWBs (not shown). Due to their larger size and duration, sustained events are likely therefore to be more effective in generating a large-scale coherent response in the oceanic thermocline then brief WWBs (Hendon *et al.* 1998).

(*b*) *Thermodynamic instability and TOVS temperature and humidity*

Figure 3 depicts raw and time-filtered fluctuations in atmospheric thermodynamic instability as judged from CAPE and GCAPE methods for sustained WWBs based on re-analysis temperature and humidity fields. The composite CAPE variation during

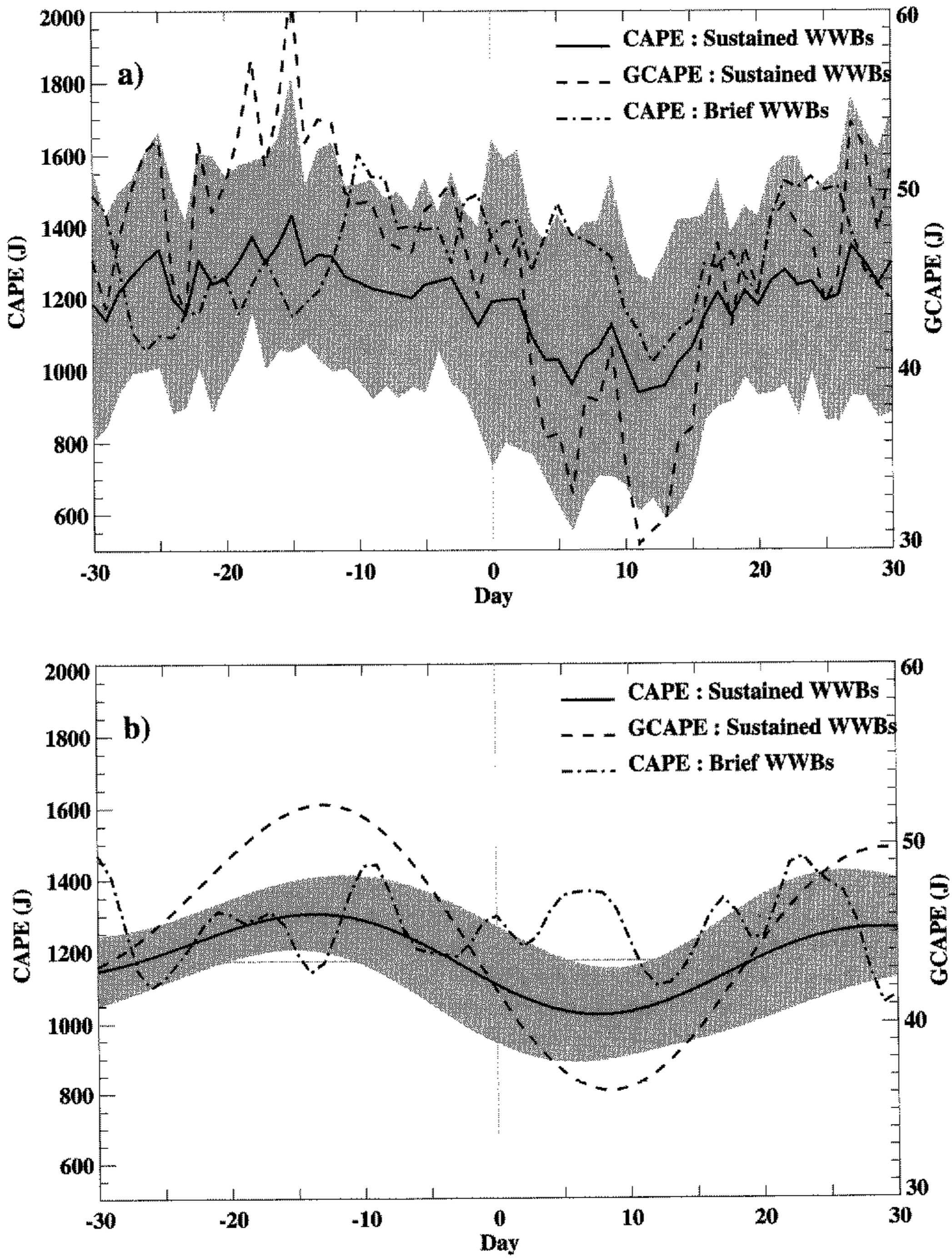

Figure 3. Composite (a) unfiltered and (b) time-filtered CAPE fluctuations from the ECMWF re-analyses for brief and sustained westerly wind bursts (WWBs). GCAPE variations for sustained WWBs also shown. Shading indicates variability among sustained CAPE events of one standard deviation above and below the mean. See text for further explanation.

brief events and the standard deviation within the distribution of sustained events are also shown. The typical variation in CAPE across Day 0 of sustained WWBs is approximately 300 J in a mean state of roughly 1150 J (26%), while the mean variation in GCAPE is approximately 15 J in a mean state of 45 J (33%). Instability is a maximum at approximately Day −14, a time following which cloud depth will be shown to increase (section 3(c)). A minimum in instability occurs at approximately Day 7 and follows a period of exceptionally strong convection. In contrast to the behaviour of sustained events, instability during brief WWBs shows no significant systematic variation (<50 J) with respect to Day 0. Tendencies in instability depicted by CAPE and GCAPE are similar as both are largely driven by changes in the moist and thermal properties of the lower troposphere (below approximately 850 hPa). Similarly, variability in instability over time is largely controlled by fluctuations in low-level humidity and temperature.

The existence of strong and consistent variations in CAPE during sustained WWBs raises many questions, however. As cloud processes in the re-analysis can significantly alter the moist and thermal structure of the atmosphere, yet confidence in their accuracy is not high (Kalnay *et al.* 1995), is the signal in CAPE an artificial result of the re-analyses' model physics or is evident in nature? If the signal in CAPE represents nature, does CAPE play a causal role in the phenomenon or is variation in CAPE merely a by-product of the processes that independently drive sustained WWBs? To begin to address these questions, satellite products from TOVS will be examined to estimate fluctuations in temperature and moisture of the lower troposphere from a data source independent of the NCEP model physics. Limitations and concerns regarding the diagnosis of CAPE's causal role will then be discussed.

Figure 4 displays composite anomalies in TOVS retrieved 900 hPa temperature and precipitable water during sustained WWBs. Variability among composited sustained events and anomalies during brief WWBs are also shown for comparison. The retrievals represent variations averaged through approximately the lower 200 hPa of the troposphere and support the diagnosis of instability from the re-analysis models. TOVS estimates show a warming and moistening of the lower troposphere followed by a period of cooling and drying that is consistent with depictions of the re-analyses. The magnitude of peak-to-trough variations in temperature and precipitable water is small, at approximately 0.6 K and 0.25 mm in the layer from 1000 to 800 hPa, but are comparable with those represented by the re-analysis. As already discussed, the variations also realize a nonlinear impact (30%) on the buoyant energy available for convection. The existence of sizable variations in CAPE during sustained WWBs therefore is probably representative of nature.

However, it is difficult to define conclusively the role of convective instability in the triggering and maintenance of sustained WWBs. Simple experiments based on the competition between radiative and convective processes (e.g. Hu and Randall 1994, 1995) suggest that intraseasonal convective variability may be governed by the development and destruction of latent instability by deep convection. However, these studies imply the existence of a threshold in instability that determines the transition from suppressed to convective conditions. No threshold in instability at the onset of WWBs is apparent (e.g. Fig. 3) as the large-scale instability at Day −10 can vary by as much as 500 J among the identified WWBs. It is possible that intraseasonal convective variations may occur independent of thermodynamic forcing such as proposed by wave-CISK* (e.g. Lindzen 1974) and that fluctuations in CAPE are the response of stability to

* Conditional Instability of the Second Kind.

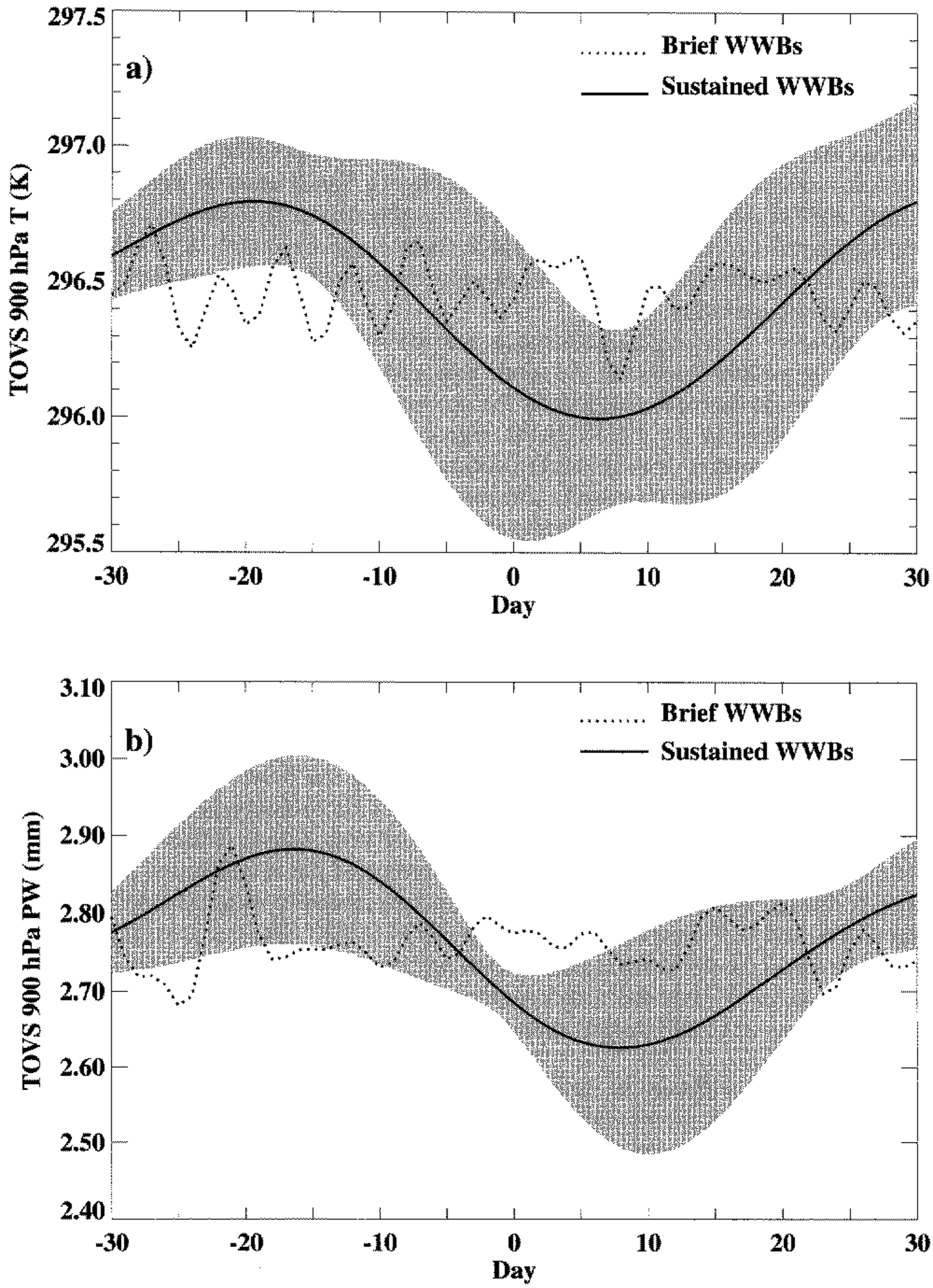

Figure 4. Composite time-filtered fluctuations in lower troposphere (900 hPa) of (a) temperature and (b) precipitable water (PW) from the TOVS (see text) for brief and sustained westerly wind bursts (WWBs). Shading indicates variability among sustained events of one standard deviation above and below the mean.

the dynamically driven variations in low-level convergence. Recently, however, another consideration has emerged as it has been found that sizable instrument-related biases (~10 to 20%) may exist in the radiosonde humidity record (Zipser and Johnson 1998; Cole 1998). The influence of the biases on the re-analysis products and the calculation of CAPE, such as in Fig. 3, is potentially large and exceedingly difficult to determine as instrumentation error and its inclusion in the assimilation process can vary in time. Due to the large sensitivity of CAPE estimates to errors in lower-tropospheric humidity, which is shown by Zipser and Johnson (1998) to be as much as 1000 J, and in light of the potentially large magnitude of the instrument biases (2 to 3 g kg^{-1}), it is probably not possible to make a definitive diagnosis regarding the role of convective instability in the triggering of sustained WWBs using the existing radiosonde record.

(c) *Cloud and precipitation anomalies*

The motions associated with tropical deep convection vertically redistribute moist and thermal energy and, as a consequence, alter atmospheric stability. Clouds and precipitation are also important because, among other effects, they play a significant role in determining the lateral heating gradients associated with radiation and condensation which force the large-scale circulation both in the mean and during its variability. Figure 5 summarizes composite fluctuations in ISCCP estimated cloud thickness (Fig. 5(a)), cloud-top pressure (P_c, Fig. 5(b)), and cloud amount (Fig. 5(c)) over the IFA for both brief and sustained WWBs. A significant enhancement in cloud optical depth (~50%) and amount (~30%) coincides with a reduction in cloud-top pressure (−20%) in the week preceding Day 0. Cloud variations suggest an increase in convective intensity during CAPE depletion (Fig. 3). The decrease in cloud-top pressure and increase in optical depth also imply a significant modulation within the cloud distribution.

To examine further the association of deep and shallow clouds with variation in CAPE (Fig. 3) and boundary-layer properties (Fig. 4), the variation of cloud amount by P_c during WWBs is shown in Fig. 6. Raw ISCCP values represent the real percentage of the IFA observed to be cloudy from satellite where P_c lies between the specified lower and upper pressure levels. Assuming a random overlap of clouds, actual cloud fraction by level can also be derived, as observed cloud per cent at a given level is equal to the amount observed from satellite divided by the percentage of sky visible at that level. For large-scale estimates over the tropics, the random-overlap assumption is probably reasonable (e.g. Bergman and Hendon 1999) though it is principally a lack of observations which prevents a more accurate diagnosis.

To help interpret the change in clouds during WWBs, the climatological distribution of clouds over the IFA is first examined. The total cloud amount over the IFA is approximately 75% as seen from the vertical integral of raw ISCCP cloud fraction (Fig. 6(a)). The annual mean distribution of cloud amount by P_c with correction for cloud overlap reveals a diverse filigree of cloud types over the IFA. Most frequent are low clouds where P_c lies between 680 and 800 hPa (~30%); however, cloud amount in other layers deep into the troposphere is also substantial (>15%). Therefore, though studies of OLR have shown that WWBs are associated with the highest cloud types, the full response in the cloud field is likely to be considerably more complex than in high clouds alone.

The response of the distribution of cloud amount by P_c is shown in Figs. 6(b) and 6(c) for brief and sustained WWBs respectively. Contours in Figs. 6(b) and 6(c) represent the change in per cent cloudiness in each pressure level (Fig. 6(a)). Again, adjustment has been made for the effect of cloud overlap. The most notable anomaly during brief WWBs occurs centred about Day −1 with an intensification of clouds

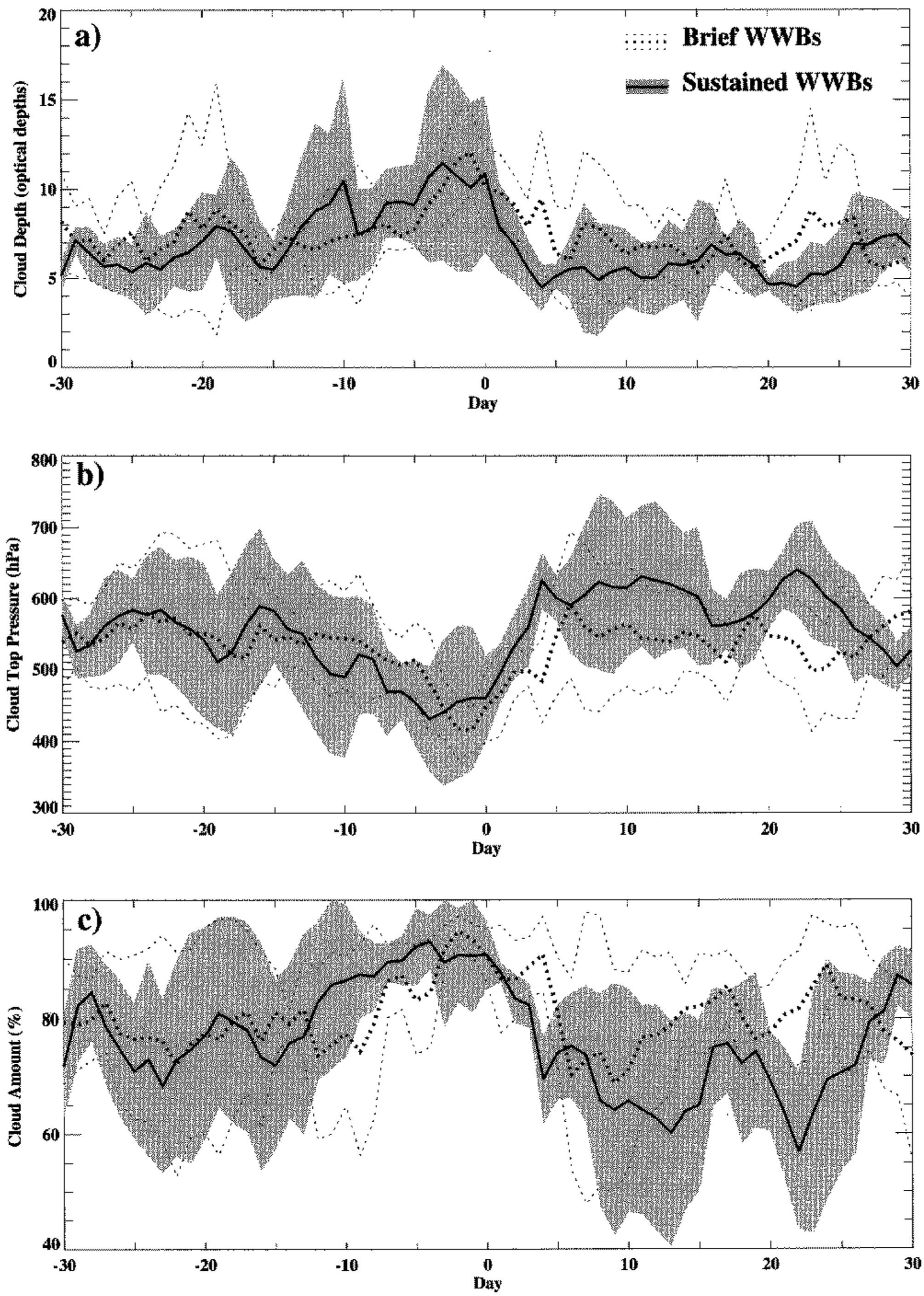

Figure 5. Composite evolution of ISCCP estimated (a) cloud optical depth, (b) cloud-top pressure, and (c) cloud amount during brief and sustained westerly wind bursts (WWBs). Dotted and shaded curves span +/− one standard deviation of the distribution of brief and sustained events respectively.

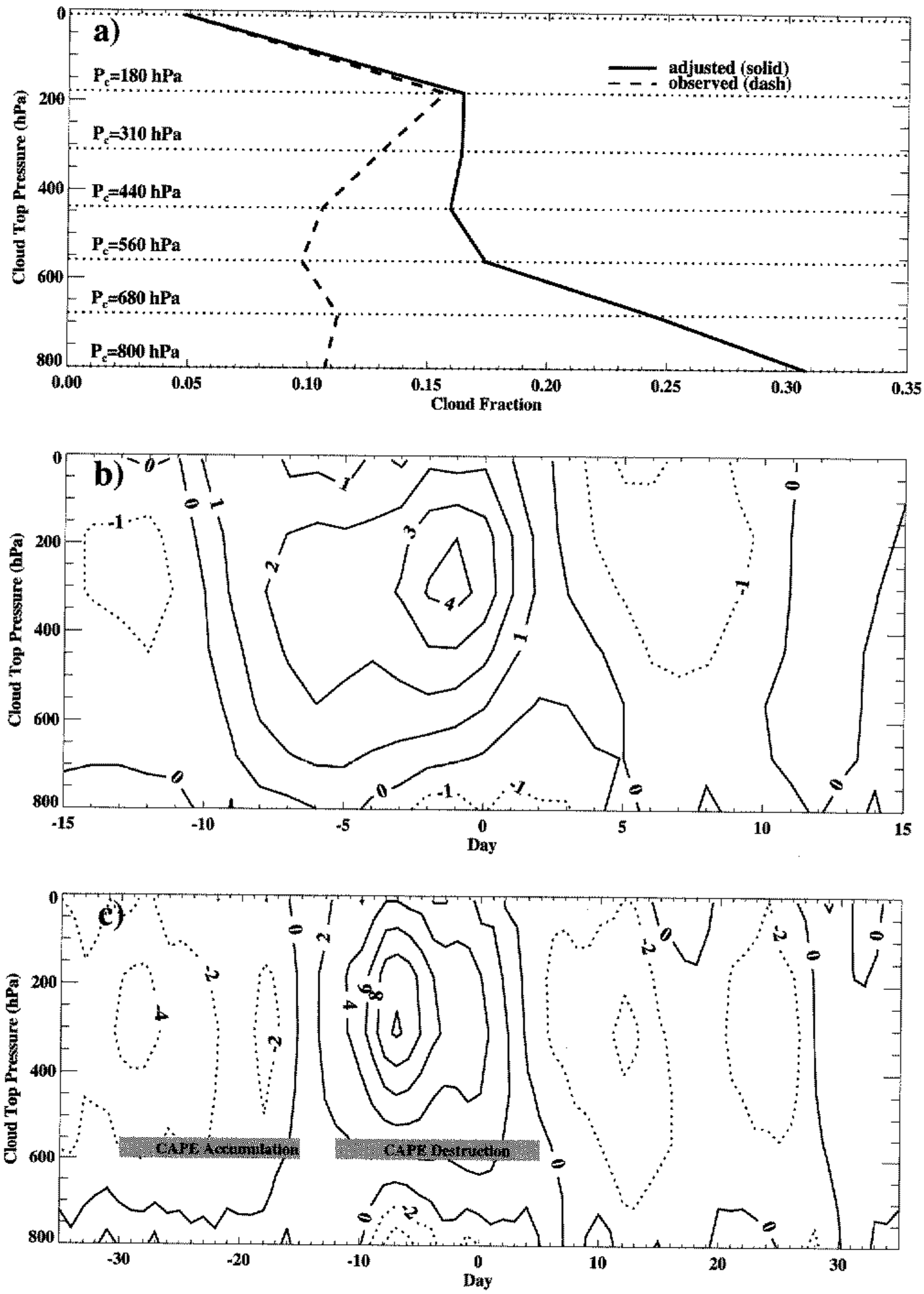

Figure 6. (a) The mean distribution of cloud-top pressure, P_c, over the intensive flux array (see text for further explanation) with composite cloud amount anomalies for (b) brief and (c) sustained westerly wind bursts (WWBs) respectively. Also indicated in (c) is the overall convective available potential energy (CAPE) tendency for sustained WWBs from Fig. 3. Negative values are shown as dashed lines.

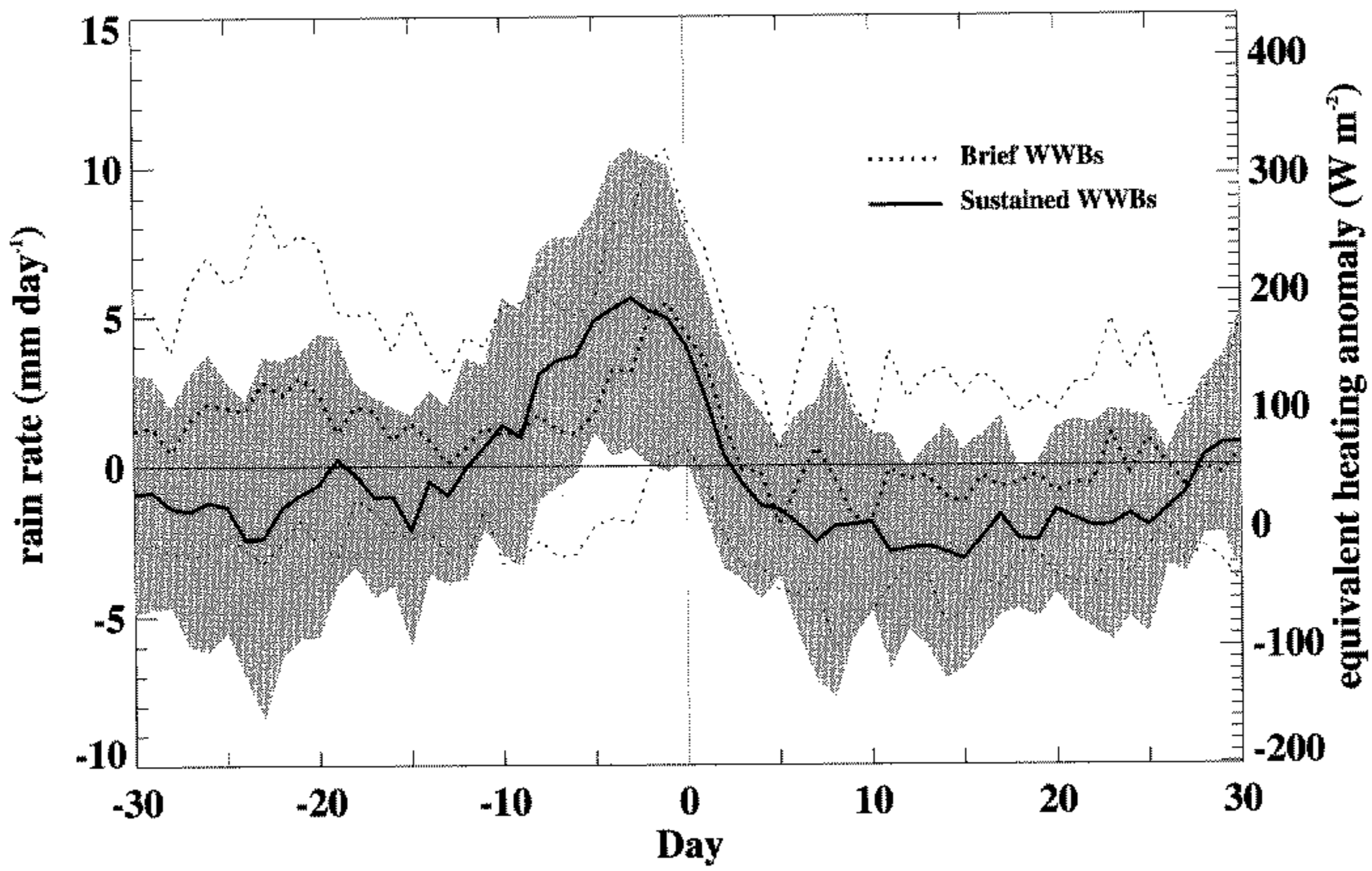

Figure 7. Composite evolution of Microwave Sounder Unit estimated rainfall for brief and sustained westerly wind bursts (WWBs). Variability among sustained and brief events of +/− one standard deviation is indicated (by shading and dotted curves respectively).

throughout the middle and upper troposphere of 2 to 4%. Reduced cloud per cent is also apparent at Day −13 and Day 7 although its magnitude is small (~1%). Variation in low cloud amount is also small during brief WWBs. Sustained WWBs experience variability in middle and upper-level cloud amount approximately twice as large (6 to 8%) as for brief WWBs, and the phase lag between clouds and winds is substantial (~8 days). A moderate (2 to 4%) reduction in low cloud is also apparent during the most intense convection. From satellite observations alone, it is not possible to deduce whether the reduction in low clouds is realistic or whether it results from an incorrect assumption of random-cloud overlap, and definitive conclusions regarding low cloud variability are not therefore possible.

Also shown in Fig. 6(c) are the periods of CAPE accumulation and destruction (Fig. 3). A coincidence of enhanced (reduced) high cloud amount with destruction (creation) of CAPE is apparent. *In-situ* studies of the interactions between the surface, boundary layer, and deep convection (e.g. Parsons *et al.* 1994; Young *et al.* 1995; Lau and Sui 1997, and others) reveal an association between deep convective clouds and convective outdraughts that cool and dry the boundary layer on the mesoscale over the time-scale of a day. Figure 6(c) supports the generalization of results from these *in-situ* studies to the larger and longer scale during the organized and prolonged convective anomalies associated with sustained WWBs.

While clouds contribute significantly to the atmospheric radiative heating anomalies associated with WWBs, diabatic heating associated with precipitation also experiences substantial variability across the life cycle of WWBs. The composite mean evolution of MSU diagnosed precipitation anomalies during WWBs is summarized in Fig. 7. The range of one standard deviation of events within each composite is also shown for sustained and brief events. At its peak in the week preceding Day 0, precipitation anomalies

typically equal the climatological mean (6 mm day^{-1}) for both brief and sustained WWBs, and correspond to an atmospheric heating anomaly of almost 200 W m^{-2}. Precipitation anomalies are longer lived for sustained WWBs than brief WWBs. Within a few days of Day 0, rainfall anomalies are typically at or below zero. During sustained WWBs, rainfall is typically below normal until more than three weeks after Day 0. Thus, the evolution of mid- and upper-tropospheric clouds (Fig. 6), and the heating anomalies they imply, are in phase with fluctuations of precipitation both substantially before and after Day 0.

(*d*) *Surface heat-flux anomalies*

The total surface energy balance comprises fluxes due to evaporation, radiation, and sensible heat. Surface flux variations over the warm pool on intraseasonal time-scales are dominated by changes in solar radiation and evaporation (e.g. Lau and Sui 1997; Fasullo and Webster 1999). Figure 8 displays evaporative and solar-flux deviations from their climatological mean during brief and sustained WWBs. The total surface energy-balance anomaly and its time integration are shown. The period over which flux anomalies are integrated is based on the duration of wind-speed anomalies greater than 1 m s^{-1} at the surface (Fig. 2). Solar-flux estimates are based on radiative modelling of ISCCP retrieved clouds (Bishop *et al.* 1997) while other flux terms are taken from the NCEP/NCAR re-analysis. These estimates have been shown to serve as suitable flux measurements for the surface energy-balance (Fasullo and Webster 1999). Turbulent-flux estimates from the ECMWF exhibit a slight (<10%) difference from those of the NCEP/NCAR re-analysis.

Typical peak-to-trough variability in latent flux is 30 to 40 W m^{-2} for brief and sustained WWBs, respectively. Solar flux variations are smaller than those in evaporation, at approximately 25 and 35 W m^{-2}, and are induced by increased cloud thickness and per cent. Evaporative variations, in contrast, are driven largely by enhanced surface wind speed (e.g. Liu *et al.* 1994). As a result, surface solar forcing is largely in phase with surface winds during brief WWBs but leads surface winds by almost a week during sustained WWBs. The integration of the total surface energy balance suggests that both brief and sustained WWBs exert an important influence on the heat content of the upper ocean, with a typical net thermal forcing of 2×10^7 to 4×10^7 J m^{-2}, respectively. SST cooling of 0.5 to 1 degC is not unusual during WWBs (McPhaden *et al.* 1988, 1992). The cooling effect of flux anomalies during sustained WWBs is partially offset by a period of warming (Day −30 to −15) during a time of high solar insolation and reduced evaporation. It is therefore likely that the enhanced diurnal cycle of SST is an important aspect of air–sea heat exchanges in the precursory warming stage of sustained WWBs (Webster *et al.* 1996). This effect is not, however, captured by the data products used in the current analysis and may need to be considered for a comprehensive assessment of the surface energy balance.

4. Composite large-scale anomaly fields during sustained WWBs

The large-scale variation of OLR and winds associated with the MJO is well documented (Madden and Julian 1994) and involves an eastwards propagation of convective and dynamic anomalies across the equatorial Indian and Pacific Oceans at a speed of roughly 5 m s^{-1}. Sustained WWBs coincide with the wet phase of the MJO (Table 2), and the large-scale relationships among CAPE, precipitation, and 850 hPa winds during these events are shown in Fig. 9. The onset period (Day −12 to −4) is

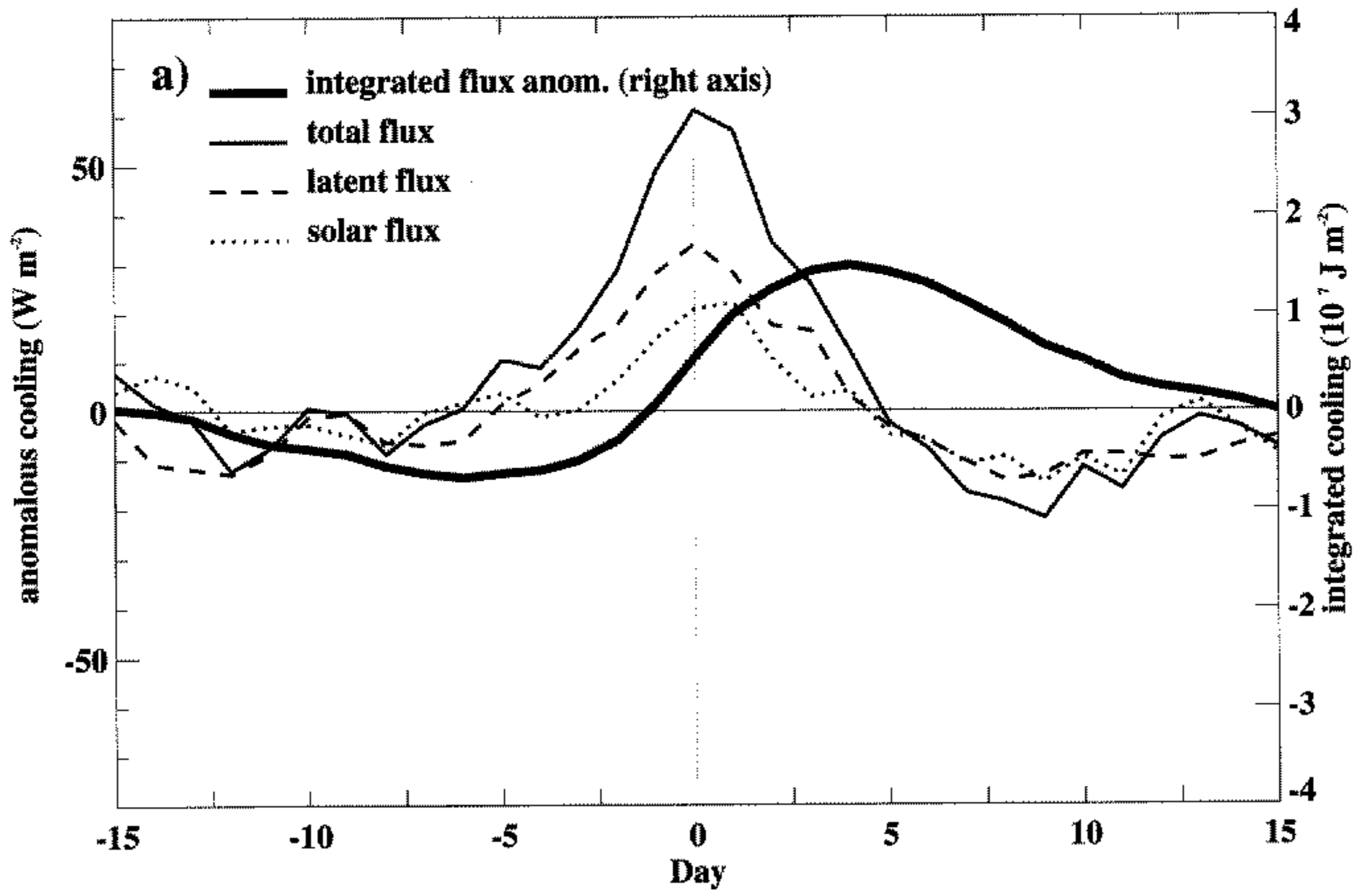

Figure 8. Composite surface heat fluxes for (a) brief and (b) sustained westerly wind bursts. Net solar, latent, total, and integrated heat fluxes are shown. Positive flux anomalies correspond to surface cooling for all terms.

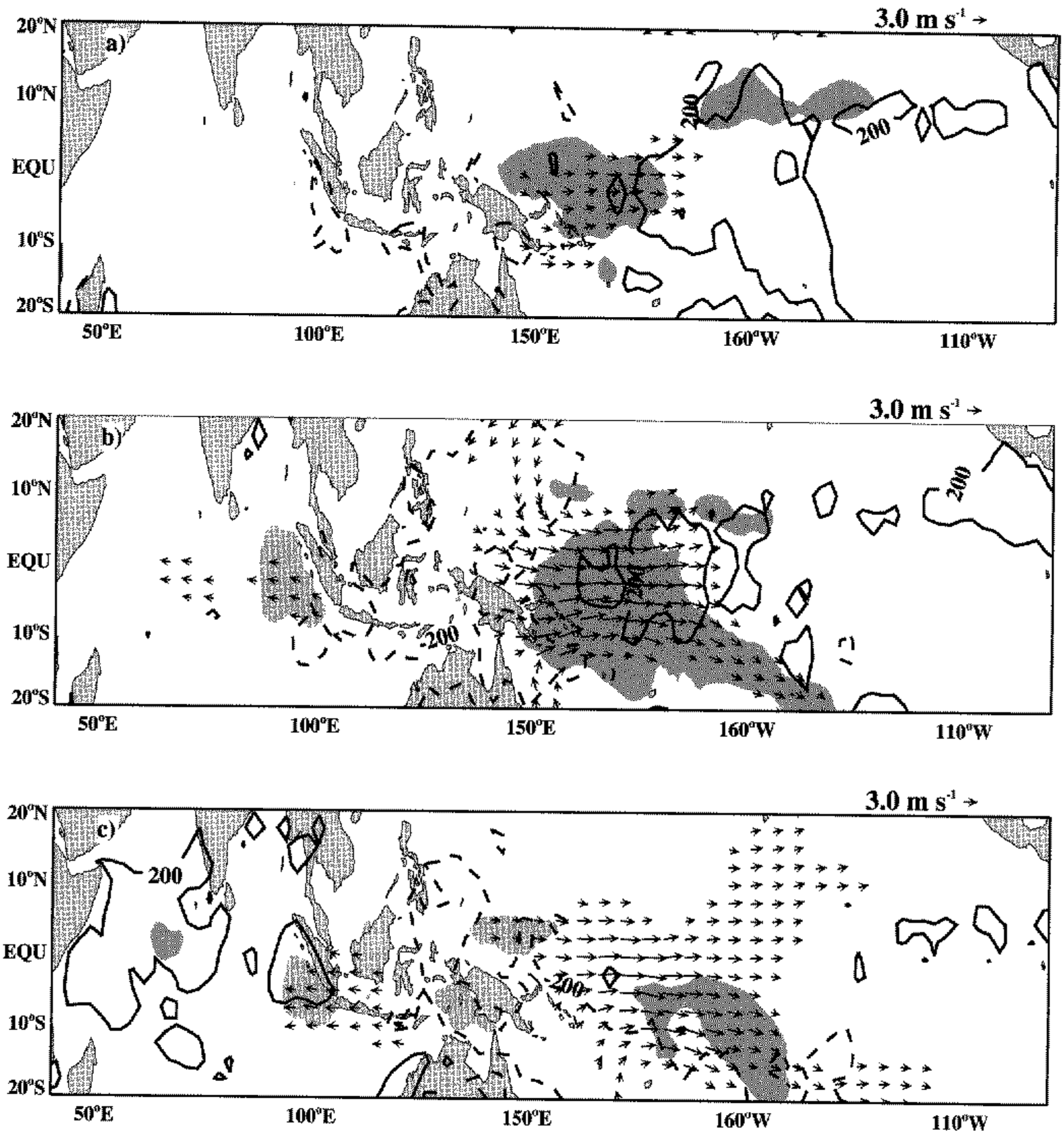

Figure 9. Large-scale 850 hPa wind (vectors), precipitation, and convective available potential energy (CAPE) anomalies during three periods about Day 0 for sustained westerly wind bursts. (a) Day −12 to Day −4, (b) Day −4 to Day +4, and (c) Day 4 to Day 12. CAPE anomalies of 200 J (solid contours) and −200 J (dashed contours) are shown for positive (solid) and negative (dashed) departures from the climatological mean. Positive (negative) precipitation anomalies of 3 mm day^{-1} are shown by the dark (light) shading.

characterized by CAPE anomalies of well over 200 J covering an expansive portion of the central Pacific Ocean. Simultaneous CAPE anomalies over the IFA have begun to diminish (Fig. 3) and negative anomalies over western Indonesia are apparent. Deep convective and westerly wind anomalies emerge over the IFA (see also Fig. 5). At the peak of the bursts (Day −4 to 4), CAPE anomalies are reduced in extent and magnitude as precipitation moves eastwards and begins to cover a large portion of the western Pacific. Westerly winds strengthen over the western Pacific Ocean and equatorward winds converge to the west of enhanced precipitation (near 150°E). Associated with the equatorward flow are negative anomalies in CAPE that may result from both convection, as already discussed, and the reduced moisture content of the dry subtropical flow

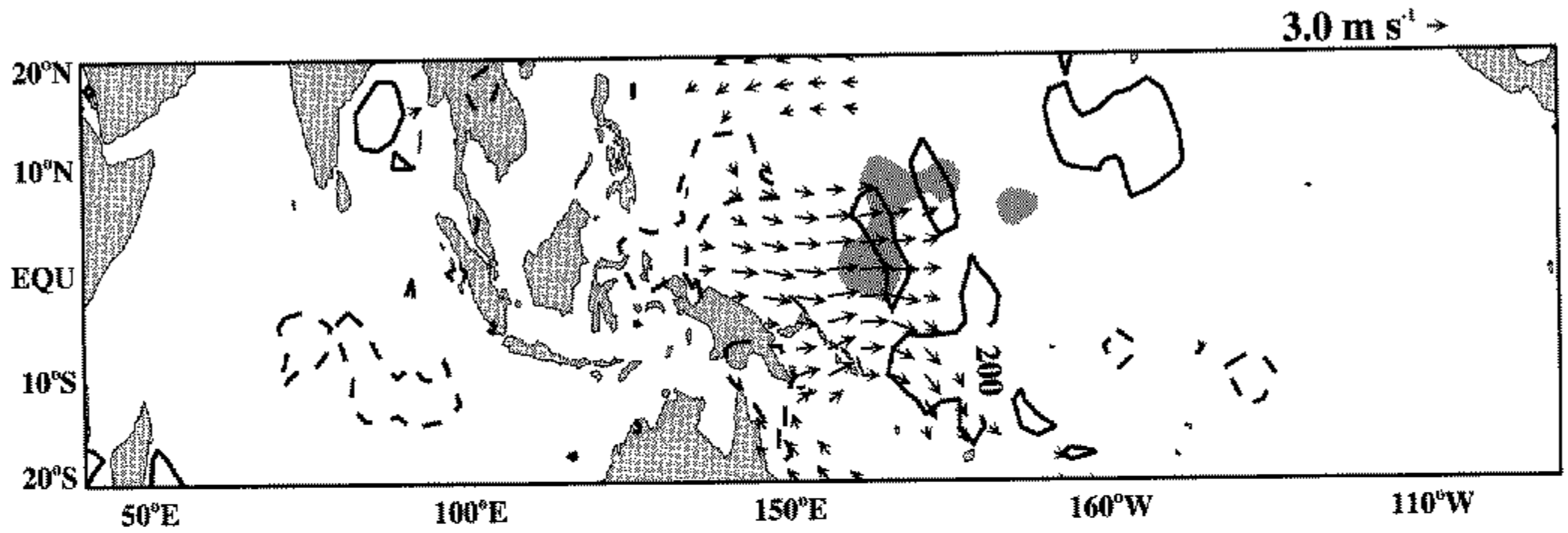

Figure 10. As in Fig. 9, but at Day −4 to Day 4 for brief westerly wind bursts.

(e.g. Brown and Zhang 1997). Easterly wind anomalies emerge over the eastern Indian Ocean and low-level zonal flow near Indonesia diverges, coinciding with negative CAPE anomalies (<−200 J). From Day 4 to 12, positive CAPE anomalies are confined to isolated regions of the eastern Pacific and western Indian Oceans while instability is reduced in the western Pacific. Widespread westerly wind anomalies persist and exhibit broad meridional extent in both hemispheres while anomalies in precipitation are confined to the south central Pacific Ocean as often associated with the MJO (Matthews *et al.* 1996). The western Indian Ocean is characterized by continued easterly wind and emerging positive CAPE and precipitation anomalies.

Many large-scale associations of sustained WWBs are absent from composites of brief WWBs; however, Day 0 shares several characteristics seen in Fig. 9. Figure 10 shows the distribution of winds, rainfall, and CAPE for Day −4 to Day 4 of brief WWBs. In contrast to sustained WWBs, CAPE anomalies exist in phase with precipitation anomalies, rather than in quadrature. Though no signature in CAPE is apparent locally over the warm pool, CAPE at the eastern extreme of westerly winds is elevated during brief WWBs but depressed at their western extreme. A similar feature was noticed during sustained WWBs. In both instances, the CAPE fluctuations are consistent with the impact of advection and divergence in the lower troposphere as positive CAPE anomalies exist in areas where warm moist air from the warm pool converges over cooler ocean, and negative CAPE anomalies exist where dry, subtropical air is advected equatorwards near the divergent western fringe of westerly wind anomalies. Aspects of CAPE variability and the roles played by clouds, advection, and divergence will now be discussed in greater detail.

5. Discussion

(*a*) *Mechanisms of CAPE variability*

Figure 11 summarizes the phase relationships between anomalies in CAPE, cloud optical depth, precipitation, and winds during sustained WWBs and suggests an important coupling of the thermodynamic and dynamic variations. The time series in Fig. 11 have been created by normalizing the time-filtered composite time series by their peak values. The apparent interaction of convection and instability is analogous to results from field studies of mesoscale convective systems but on much larger spatial and temporal scales. Variations in CAPE lead those in precipitation and clouds by approximately a quarter cycle and suggest that, before the convective outbreaks of sustained WWBs, an

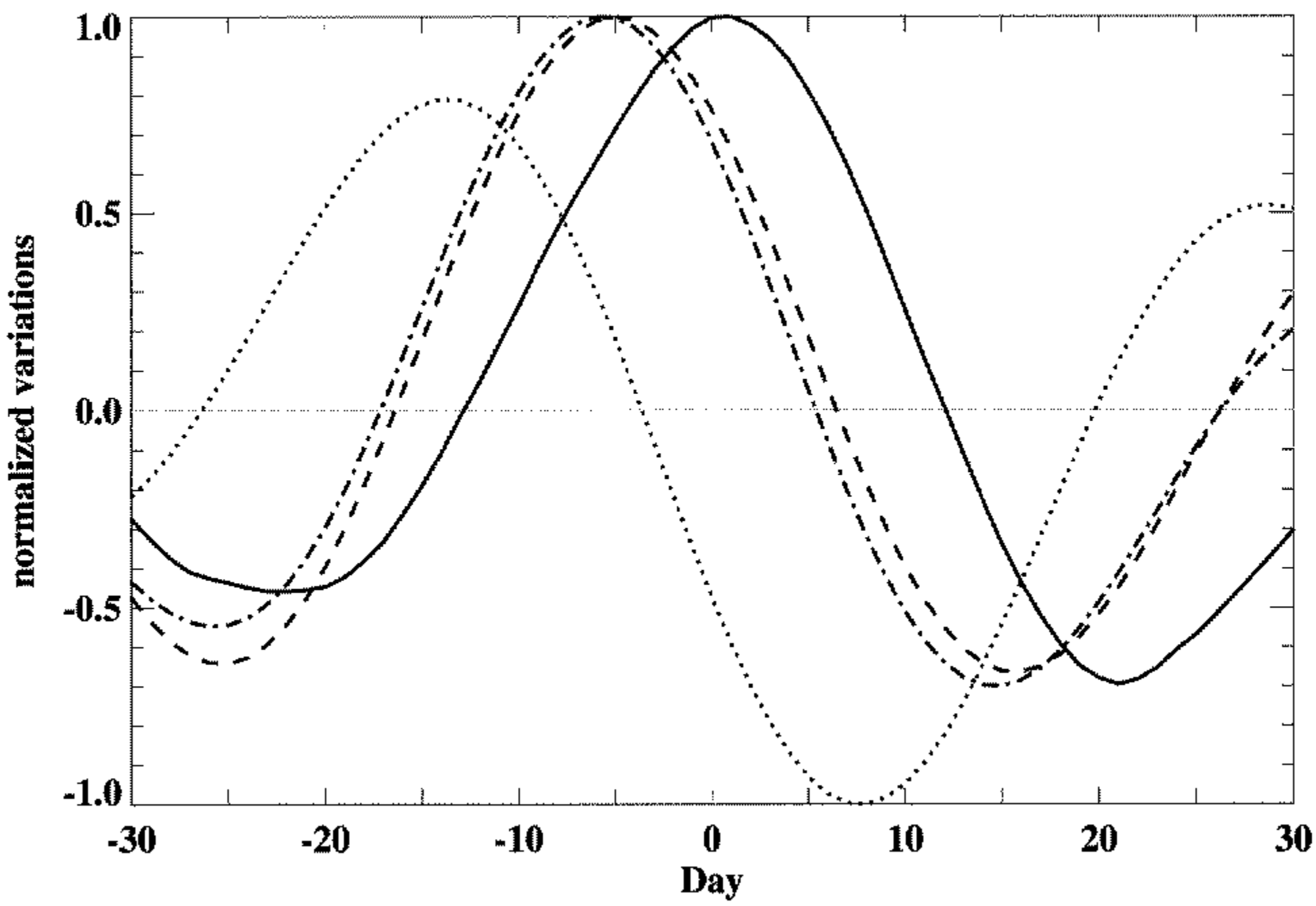

Figure 11. Phase relationship between time-filtered composite convective available potential energy (CAPE) (dotted), cloud optical depth (dash-dotted), rainfall (dashed), and westerly wind (solid) anomalies during sustained westerly wind bursts. The time series are normalized by their maximum values.

environment favourable to convection is established. During the period in which CAPE anomalies are positive, clouds deepen and rainfall strengthens, together acting to cool and dry the atmosphere's lower layers (Fig. 4) despite enhanced surface evaporation (Fig. 8). It is likely that convective wakes, the dry and cool convective out-draughts that are often associated with tropical deep convection, play an important role in stabilizing the atmosphere, even over very long temporal and very large spatial scales. Convective wakes have been observed in both the TOGA-COARE (Young *et al.* 1995) and the GARP (Global Atmospheric Research Program) Atlantic Tropical Experiment (GATE) (Seguin and Garstang 1976; Zipser 1977) field campaigns, and though limited in spatial extent, wakes can modulate collectively large-scale characteristics of the lower atmosphere. Quantitative results from GATE show that during periods of widespread convection, 30% of the tropical Atlantic Ocean is directly influenced by convective wakes (Gaynor and Mandics 1979). In such regions, the energy available to deep convection is reduced by up to 60% (Barnes and Garstang 1982) and is similar to the peak-to-trough variation of GCAPE seen in the raw composite sustained WWB (Fig. 3).

Advection and divergence in the lower troposphere may also contribute importantly to variations in CAPE during brief and sustained WWBs (Figs. 9 and 10). Positive CAPE anomalies at 170°E are consistent with convergence of moisture at the leading edge of westerly anomalies, while negative anomalies are located at the divergent western extreme of the anomalies, where advection from the subtropics is also apparent. Case-studies of the 31 December 1992 event (Fig. 1; Sheu and Liu 1995; Brown and Zhang 1997) show that midtropospheric (500 hPa) advection can act to establish a dry atmospheric layer that may subsequently inhibit convection. Brown and Zhang (1997) maintain that the intrusion of these dry layers plays a causal role in the decay of convection and that such variations are more important than boundary-layer fluctuations

in modulating convection. Case-studies remain limited in their ability to characterize WWBs as a group however. Moreover, intrusion of midtropospheric dry layers over the IFA is not consistently evident in the re-analysis products during the composite WWBs of the present study. Rather, widespread drying as depicted by the re-analysis products originates in the lower troposphere (850 hPa) and extends aloft over several days. Over the eastern extreme of the warm pool and the maritime continent, however, changes in CAPE are consistent with advection and divergence in the lower troposphere. Thus, it is probable that advection, divergence, and convection play important roles in modifying atmospheric stability and that their relative importance may vary with location. There may also be limits in resolving such issues with re-analysis data, however, due to the limited vertical resolution of the re-analysis models and their input data, and the potentially fine scale of dry intrusions. Observations of water vapour included in the assimilation process over open ocean (e.g. satellite retrievals) are typically coarse in vertical resolution. Final determination of the relative importance of advection, divergence, and convection may be best accomplished in a separate analysis of rawinsonde observations over an extended climatology, though a significant challenge for such an analysis may be posed by biases in the existing rawinsonde record.

(*b*) *Implications for theoretical descriptions of the MJO*

The strong coincidence between sustained WWBs and the active phase of the MJO allows comparison of composite sustained WWBs with theories of tropical intraseasonal variability. Wind-Induced Surface Heat Exchange (WISHE, Emanuel 1987; Neelin *et al.* 1987) modes of variability require that intraseasonal variations occur in a basic state of low-level easterly winds and that low-level easterly anomalies induce elevated surface heat fluxes and precipitation. The WISHE mechanism explains both the development and propagation of the MJO from these constraints. Aspects of WISHE are at odds with the behaviour of WWBs, however, as negative surface evaporative flux anomalies accompany surface easterlies and reduced convection. Rather, it is the westerly phase of surface winds (i.e. those during WWBs), in which large evaporation and precipitation anomalies occur (Figs. 7, 8, 9 and 11).

Kelvin-wave CISK explanations of the MJO rely on dry Kelvin-wave dynamics and require anomalies in convection and winds to be centred about the equator (e.g. Hendon 1988). Further, as low-level convergence is driven by the large-scale wave pattern, convection is collocated with the convergent focus of low-level easterly and westerly winds. Interactions between wave dynamics and diabatic heating associated with convection slow the phase speed of the disturbances and contribute to a bias of convection toward surface westerlies (e.g. Hendon 1988). The composite sustained WWB shows the assertion of widespread deep convection during westerly surface winds to be reasonable. Wave-CISK explanations of the MJO are subsets of Kelvin-wave descriptions and rely on wave induced low-level convergence (Lindzen 1974; Lau and Peng 1987) to generate an environment favourable to deep convection. The large-scale distribution of CAPE, precipitation, and wind anomalies (Fig. 9) is consistent with wave-CISK as convection develops east of low-level westerly winds and follows a period of exceptionally high CAPE. However, these refinements in wave-CISK do little to explain the bias of dynamic and convective anomalies to the southern hemisphere (Fig. 9). While Kelvin-wave dynamics may explain aspects of the MJO, their ability to explain fully intraseasonal variations in the tropical western Pacific appears limited. Given the seasonality of WWBs (Table 2) and the tendency of MJO convection to propagate into regions of high climatological mean rainfall associated with the Australian monsoon (McBride 1983), a comprehensive consideration of large-scale features of the tropical

Pacific, such as its monsoon (McBride 1983) and the interaction between its heating and Rossby waves (Matthews *et al.* 1996), may be required to understand the seasonality and physical underpinnings of all classes of WWBs better.

6. Conclusions

The relationship between clouds, convective instability, and the surface energy balance during WWBs over the IFA depends strongly on the spatial and temporal scale of the events. An important distinction can be made between brief (5–25 day) and sustained (30–90 day) WWBs. Brief WWBs occur independent of the MJO during all ENSO phases and are characterized by a near simultaneous increase in clouds, precipitation, and westerly winds that extend deeply through the troposphere. Surface evaporative and solar-flux enhancements during brief WWBs are typically 30 W m^{-2} and 25 W m^{-2}, respectively, though the duration of the anomalies is short (approximately 10 days) and variations in convective instability are small. Though brief WWBs exert little influence on CAPE above the warm pool, advection and divergence associated with the events away from the warm pool contribute to modifications of CAPE.

Sustained events are strongly associated with the wet phase of the MJO during all ENSO conditions and are associated with an out-of-phase relationship between CAPE, clouds, and winds. Convective instability fluctuates by approximately 30% and elevated CAPE precedes the outbreak of convection, suggesting an important influence of the lower troposphere on the large-scale circulation and an important coupling between the dynamic and thermodynamic fields. The relationship between CAPE, sustained WWBs, and the changing distribution of clouds is investigated. The surface energy balance is assessed and both evaporative and solar-flux anomalies are found to contribute significantly to surface cooling. When integrated across the period of surface wind anomalies, flux anomalies result in approximately twice as much surface cooling during sustained bursts as during brief events. Finally, the composites aid in evaluating theoretical depictions of the MJO, though several questions remain unanswered regarding the role of thermodynamics in triggering WWBs, and interactions between WWBs, climatological mean heating, and tropospheric waves.

Acknowledgements

This study was supported by National Science Foundation (USA) Grants ATM 921 4840 and ATM 922 3150. NCAR/NCEP Re-analysis data were provided through the NOAA Climate Diagnostics Center (http://www.cdc.noaa.gov). The authors would also like to acknowledge the support of Dr Rossow of the National Aeronautics and Space Administration's Goddard Space Flight Center's Institute for Space Studies, and the assistance of Dr J. Curry and Dr G. Kiladis in reviewing the manuscript.

References

Arkin, P. and Webster, P. J. 1985 Annual and interannual variability of tropical–extratropical interactions: An empirical study. *Mon. Weather Rev.*, **113,** 1510–1523

Barnes, G. and Garstang, M. 1982 Subcloud layer energies of precipitating convection. *Mon. Weather Rev.*, **110,** 102–117

Bergman, J. W. and Hendon, H. H. 1998 Calculating monthly radiative fluxes and heating rates from monthly cloud observations. *J. Atmos. Sci.*, **55,** 3471–3492

Bishop, J. K. B., Rossow, W. B. and Dutton, E. G. 1997 Surface solar irradiance from the International Satellite Cloud Climatology Project 1983–1991. *J. Geophys. Res.*, **102,** 6883–6910

Brown, R. G. and Zhang, C. 1997 Variability of midtropospheric humidity and its effect on cloud-top height distribution during TOGA COARE. *J. Atmos. Sci.*, **54,** 2760–2774

Chang, C.-P. and Lau, K. M. 1982 Short term planetary interaction over the tropics and subtropics. Part I: Contrast between active and break periods. *Mon. Weather Rev.*, **110,** 933–946

Chu, P. and Frederick, J. 1990 Westerly wind bursts and surface heat fluxes in the equatorial western Pacific in May 1992. *J. Meteorol. Soc. Japan*, **68,** 523–537

Cole, H. 1998 'Correction and recalculation of humidity data from TOGA-COARE radiosondes and development of humidity correction algorithms for global radiosonde data'. Proceedings of the CLIVAR/GEWEX COARE98 conference. JOSS, UCAR, Boulder, CO, USA

Compo, G. P., Kiladis, G. N. and Webster, P. J. 1999 The horizontal and vertical structure of east Asian winter monsoon pressure surges. *Q. J. R. Meteorol. Soc.*, **125,** 29–54

Duchon, C. E. 1979 Lanczos filtering in one and two dimensions. *J. Appl. Meteorol.*, **18,** 1016–1022

ECMWF 1997 'ERA description'. ECMWF Re-Analysis Project Report Series, 1. European Centre for Medium-Range Weather Forecasts, Reading, UK

Emanuel, K. A. 1987 An air–sea interaction model of intraseasonal oscillations in the tropics. *J. Atmos. Sci.*, **44,** 2324–2340

Eriksen, C. C. 1993 Equatorial ocean response to rapidly translating wind bursts. *J. Phys. Oceanogr.*, **23,** 1208–1230

Fairall, C. W., Bradley, E. F., Rogers, D. P., Edson, J. B. and Young, G. S. 1996 Bulk parameterization of air–sea fluxes for TOGA COARE. *J. Geophys. Res.*, **101,** C2, 3747–3764

Fasullo, J. and Webster, P. J. 1999 Warm pool SST variability in relation to the surface energy balance. *J. Climate*, **12,** 1292–1305

Gaynor, J. E. and Mandics, C. F. 1979 Analysis of the convectively modified GATE boundary layer using *in situ* and acoustic sounder data. *Mon. Weather Rev.*, **107,** 985–993

Gibson, J. K., Kallberg, P., Uppala, S., Hernandez, A., Nomura, A. and Serrano, E. 1997 'ECMWF Re-Analysis'. Project Report Series. European Centre for Medium-Range Weather Forecasts, Reading, UK

Godfrey, J. S., Alexiou, A., Ilahude, A. G., Legler, D. M., Luther, M. E., McCreary Jr, J. P., Meyers, G. A., Mizumo, K., Rao, R. R., Shetye, S. R., Toole, J. H. and Wacongne, S. 1995 'The role of the Indian Ocean in the global climate system: Recommendations regarding the global Ocean Observing System'. Report of the Ocean Observing System Development Panel, Texas A&M University, College Station, TX, USA

Gutzler, D. S., Kiladis, G. N., Meehl, G. A., Weickmann, K. M. and Wheeler, M. 1994 The global climate of December 1992–February 1993. Part II: Large-scale variability across the tropical western Pacific during TOGA COARE. *J. Climate*, **7,** 1606–1622

Harrison, D. E. and Giese, B. 1991 Episodes of surface westerly winds as observed from islands in the western tropical Pacific. *J. Geophys. Res.*, **96,** 3221–3237

Harrison, D. E. and Schopf, P. S. 1984 Kelvin-wave-induced anomalous advection and the onset of surface warming in El Niño events. *Mon. Weather Rev.*, **112,** 923–933

Harrison, D. E. and Vecchi, G. A. 1997 Westerly wind events in the tropical Pacific, 1986–1995. *J. Climate*, **10,** 3131–3156

Hartten, L. M. 1996 Synoptic settings of westerly wind bursts. *J. Geophys. Res.*, **101** (D12), 16997–17019

Hendon, H. H. 1988 A simple model of the 40–50 day oscillation. *J. Atmos. Sci.*, **45,** 569–584

Hendon, H., Liebmann, B. and Glick, J. D. 1998 Oceanic Kelvin wave and the Madden–Julian Oscillation. *J. Atmos. Sci.*, **55,** 88–101

Hu, Q. and Randall, D. 1994 Low-frequency oscillations in radiative–convective systems. *J. Atmos. Sci.*, **51,** 1089–1099

1995 Low-frequency oscillation in radiative–convective systems. Part II: An idealized model. *J. Atmos. Sci.*, **52,** 478–490

Kalnay, E., Kanamitsu, M., Kistler, R., Collins, W., Deaven, D., Gandin, L., Iredell, M., Saha, S., White, G., Woollen, J., Zhu, Y., Chelliah, M., Ebisuzaki, W., Higgins, W., Janowiak, J., Mo, K. C., Ropelewski, C., Wang, J., Leetmaa, A., Reynolds, R., Jenne, R. and Joseph, D. 1995 The NCEP/NCAR 40-year reanalysis project. *Bull. Am. Meteorol. Soc.*, **77**, 437–471

Kiladis, G., Meehl, G. and Weikman, K. 1994 Large-scale circulation associated with WWBs and deep convection over the western equatorial Pacific. *J. Geophys. Res.*, **99**, 18527–18544

Knox, R. A. and Halpern, D. 1982 Long-range Kelvin wave propagation of transport variations in the Pacific Ocean equatorial currents. *J. Marine Res.*, **40**, 329–339

Lander, M. A. and Morrissey, M. L. 1988 'Genesis of twin typhoons associated with a west wind burst in the equatorial western Pacific: A case study'. Pp. 163–174 in Proceedings of the US TOGA western Pacific air–sea interaction workshop. Technical Report USTOGA-8, University Corporation for Atmospheric Research, Boulder, Colorado, USA

Lau, K.-M. and Peng, L. 1987 Origin of low-frequency (intraseasonal) oscillations in the tropical atmosphere. I. Basic theory. *J. Atmos. Sci.*, **44**, 950–972

Lau, K.-M. and Sui, C.-H. 1997 Mechanisms of short-term sea surface temperature regulation: Observations during TOGA COARE. *J. Climate*, **10**, 465–472

Lim, H. and Chang, C.-P. 1981 A theory for midlatitude forcing of tropical motions during winter monsoons. *J. Atmos. Sci.*, **38**, 2377–2392

Lindzen, R. 1974 Wave-CISK in the tropics. *J. Atmos. Sci.*, **31**, 156–179

Liu, W. T., Zhang, A. and Bishop, J. 1994 Evaporation and solar irradiance as regulators of sea surface temperature in annual and interannual changes. *J. Geophys. Res.*, **99**, 12623–12637

Lukas, R. and Lindstrom, E. 1991 The mixed layer of the western equatorial Pacific Ocean. *J. Geophys. Res.*, **96**, 3343–3357

Lukas, R., Hayes, S. P. and Wyrtki, K. 1984 Equatorial sea level response during the 1982–83 El Niño. *J. Geophys. Res.*, **89**, 10425–10430

Luther, D. S., Harrison, D. E. and Knox, R. A. 1983 Zonal winds in the central equatorial Pacific and El Niño. *Science*, **222**, 327–330

Madden, R. and Julian, P. 1972 Detection of a 40–50 day oscillation in the tropical Pacific. *J. Atmos. Sci.*, **29**, 702–708

1994 Observations of the 40–50 day tropical oscillation: A review. *Mon. Weather Rev.*, **122**, 814–837

Magana, V., Amador, J. A. and Medina, S. 1998 The mid-summer drought over Mexico and Central America. *J. Climate*, **12**, 1577–1588

Matthews, A. J., Hoskins, B. J., Slingo, J. M. and Blackburn, M. 1996 Development of convection along the SPCZ within a Madden–Julian oscillation. *Q. J. R. Meteorol. Soc.*, **122**, 669–688

McBride, J. L. 1983 Satellite observations of the southern hemisphere monsoon during winter MONEX. *Tellus*, **35A**, 189–197

McPhaden, M. J., Freitag, H. P., Hayes, S. P., Taft, B. A., Chen, Z. and Wyrtki, K. 1988 The response of the equatorial Pacific Ocean to a westerly wind burst in May 1986. *J. Geophys. Res.*, **93**, 10589–10603

McPhaden, M. J., Bahr, F., Penhoat, Y., Firing, E., Hayes, S. P., Niiler, P., Richardson, P. and Toole, J. 1992 The response of the western equatorial Pacific Ocean to westerly wind bursts during November 1989 to January 1990. *J. Geophys. Res.*, **97**, 14289–14303

Murakami, T. and Sumathipala, W. L. 1989 Westerly bursts during the 1982/83 ENSO. *J. Climate*, **2**, 71–85

Neelin, J. D., Held, I. M. and Cook, K. H. 1987 Evaporation wind feedback and low-frequency variability in the tropical atmosphere. *J. Atmos. Sci.*, **44**, 2341–2348

Nitta, T. and Motoke, T. 1987 Abrupt enhancement of convective activity and low-level westerly wind burst during the onset phase of the 1986–1987 El Niño. *J. Meteorol. Soc. Japan*, **65**, 497–506

Parsons, D., Dabberdt, W., Cole, H., Hock, T., Martin, C., Barrett, A. L., Miller, E., Spowart, M., Howard, M., Ecklund, W., Carter, D., Cage, K. and Wilson, J. 1994 The Integrated Sounding System: Description and preliminary observations from TOGA-COARE. *Bull. Am. Meteorol. Soc.*, **75**, 553–567

Randall, D. A. and Wang, J. 1992 The moist available energy of a conditionally unstable atmosphere. *J. Atmos. Sci.*, **49**, 240–255

Rossow, W. B. and Schiffer, R. A. 1991 ISCCP cloud data products. *Bull. Am. Meteorol. Soc.*, **72**, 2–20

Salby, M. and Hendon, H. 1994 Intraseasonal behavior of clouds, temperature, and motion in the tropics. *J. Atmos. Sci.*, **51**, 2207–2224

Seguin, W. R. and Garstang, M. 1976 Some evidence of the effects of convection on the structure of the tropical sub-cloud layer. *J. Atmos. Sci.*, **33**, 660–666

Sheu, R.-S. and Liu, G. 1995 Atmospheric humidity variations associated with westerly wind bursts during TOGA COARE. *J. Geophys. Res.*, **100**, 25759–25768

Smith, W. L., Woolf, H. M., Hayden, C. M., Wark, D. Q. and McMillin, L. M. 1979 The TIROS-N Operational Vertical Sounder. *Bull. Am. Meteorol. Soc.*, **60**, 117–118

Spencer, R. W. 1993 Global oceanic precipitation from the MSU during 1979–91 and comparisons to other climatologies. *J. Climate*, **6**, 1301–1326

Webster, P. J. and Lukas, R. 1992 TOGA COARE: The Coupled Ocean–Atmosphere Response Experiment. *Bull. Am. Meteorol. Soc.*, **73**, 1–39

Webster, P. J., Clayson, C. A. and Curry, J. A. 1996 Clouds, radiation and the diurnal cycle of sea surface temperature in the tropical western Pacific Ocean. *J. Climate*, **9**, 1712–1730

Williams, M. 1981 'Interhemispheric interaction during Winter MONEX'. Pp. 12–16 in Proceedings of the International conference on early results of FGGE and large-scale aspects of its monsoon experiments. WMO, **10**

World Climate Research Programme 1990 Proceedings of the International TOGA scientific conference, Honolulu, July 1990. WCRP-43 (WMO/TD-No. 379). Geneva, Switzerland

World Meteorological Organization 1985 'Scientific plan for the tropical ocean and Global Climate Program'. WCRP Publication Series No. 3, WMO/TD 64. Geneva, Switzerland

Wyrtki, K. 1975 El Niño—the dynamic response of the equatorial Pacific Ocean to atmospheric forcing. *J. Phys. Oceanogr.*, **15**, 572–584

Young, G., Ledvina, D. and Fairall, C. W. 1992 Influence of precipitating convection on the surface energy budget observed during a TOGA pilot cruise in the tropical western Pacific Ocean. *J. Geophys. Res.*, **97**, 9595–9603

Young, G., Perugini, S. and Fairall, C. W. 1995 Convective wakes in the equatorial western Pacific during TOGA. *Mon. Weather Rev.*, **123**, 110–123

Zipser, E. J. 1977 Mesoscale and convective-scale downdraughts as distinct components of squall line structure. *Mon. Weather Rev.*, **105**, 1568–1589

Zipser, E. J. and Johnson, R. H. 1998 'Systematic errors in radiosonde humidities: A global problem?' In 10th Symposium on meteorological observations and instrumentation, 11–16 January 1998, Phoenix, AZ, USA (Available from the American Meteorological Society, 45 Beacon St., Boston, MA, 02108–3693, USA)